Amphiregulin mediates non-cell-autonomous effect of senescence on reprogramming

Mathieu von Joest[1,3], Cheng Chen[1], Thibaut Douché[2], Aurelie Chiche[1], Mariette Matondo[2], Han Li[1*]

[1] *Cellular Plasticity & Disease Modelling,*

Dept. of Developmental & Stem Cell Biology, CNRS UMR 3738

[2] *Proteomics Platform, Mass Spectrometry for Biology Unit (MSBio), USR CNRS 2000,*

Institut Pasteur, 25 rue du Dr Roux, Paris 75015, France

[3] *Current address*: *Laboratory of chromatin and gene regulation during development, Imagine Institute, INSERM UMR1163, 75015, Paris, France*

* *Correspondence*: Han Li

Institut Pasteur,

25 rue du Dr Roux, Paris 75015, France

Tel: +33 (0)1 45 68 8484

Fax: +33 (0)1 45 68 8963

Email: han.li@pasteur.fr

Key words: cellular senescence / SASP/ in vitro & in vivo reprogramming / cellular plasticity / amphiregulin

Running title: Senescence-associated amphiregulin modulates reprogramming

Cellular senescence is an irreversible growth arrest with a highly dynamic secretome, termed the senescence-associated secretory phenotype (SASP). Senescence has been implicated in somatic reprogramming to pluripotency. The cell-intrinsic proliferation arrest is a barrier for reprogramming, whereas the SASP facilitates the cell fate conversion in nonsenescent cells. However, the mechanisms by which reprogramming-induced senescence regulates cell plasticity are not well understood. Here, we have further investigated how the heterogeneity of paracrine senescence impacts reprogramming. We show that senescence promotes *in vitro* reprogramming in a stress-dependent manner. We identified a catalog of SASP factors and pathways potentially involved in the cell fate conversion using an unbiased proteomic analysis. Amphiregulin (AREG), a growth factor frequently secreted by the senescent cells, promotes *in vitro* reprogramming by

accelerating proliferation and MET via the EGFR signaling pathway. Of note, AREG treatment diminished the negative effect of donor age on reprogramming. Finally, AREG enhances *in vivo* reprogramming in the skeletal muscle. Hence, senescence could facilitate cellular plasticity via various SASP factors to promote reprogramming and tissue repair.

BACKGROUND

Cellular senescence is a stress response characterized by a permanent cell-cycle arrest, acquisition of a senescence-associated secretory phenotype (SASP), and resistance to apoptosis (Hernandez-Segura et al., 2018). Senescence is involved in variety biological and pathological processes including development, tissue repair, tumorigenesis, and organism aging (Munoz-Espin and Serrano, 2014; Rhinn et al., 2019). Of note, SASP plays a crucial role in mediating senescence non-cell autonomous functions by interacting with neighboring cells and the surrounding microenvironment (Ito et al., 2017). It is becoming clear that senescence phenotypes, particularly SASP composition, are highly heterogeneous and depending on the initial stimuli, the affected cell type, and the anatomic location (Hernandez-Segura et al., 2017) (Ito et al., 2017).

Cellular reprogramming is a process of converting fully differentiated cells back to the pluripotent state, which has tremendous potentials in many areas of biomedical research (Takahashi and Yamanaka, 2006; Robinton and Daley, 2012). Interestingly, recent studies revealed that senescence has both cell-autonomous and non-cell-autonomous effects on reprogramming (Aarts et al., 2017; Banito et al., 2009; Chiche et al., 2017; Mosteiro et al., 2016; Mosteiro et al., 2018). Ectopic expression of reprogramming factors: Oct4, Klf4, Sox2, and c-Myc (OSKM), induced senescence as a cell intrinsic barrier for reprogramming (Banito et al., 2009), which in turn promote cellular plasticity and reprogramming in the non-senescent cells via SASP, in particularly by interleukin-6 (IL-6) (Chiche et al., 2017; Mosteiro et al., 2016; Mosteiro et al., 2018). However, the mechanisms by which paracrine senescence, with specific SASP factor(s), regulate cellular plasticity in the context of reprogramming remain not fully understood.

The epidermal growth factor receptor (EGFR) signaling pathway is one of the most important pathways that regulate cellular growth, proliferation, differentiation, and survival (Herbst, 2004). Although it is important for embryonic stem cells functions (Schuldiner et al., 2000; Yu et al., 2019) and the early embryonic development (Kim et al., 1999), the role of the EGFR signaling pathway in somatic reprogramming remains poorly understood. A variety of senescent cells produce abundant amphiregulin (AREG) (Coppe et al., 2010), a low-affinity EGFR ligand (Jones et al., 1999; Shoyab et al., 1988). Of note, accumulating evidence indicates AREG is a vital mediator of the immune response in infection and tissue repair (Zaiss et al., 2015). It has been suggested that AREG regulates senescence (Pommer et al., 2021) and contributes to an immunosuppressive tumor microenvironment

75 (Xu et al., 2019). Given the pleiotropic functions of AREG, its roles in mediating senescence functions
76 remain largely unexplored.
77
78 In this study, we investigated how paracrine senescence impacts reprogramming focusing on the stress
79 dependent SASP heterogeneity and identified a collection of SASP factors potentially important for
80 cellular plasticity using unbiased proteomic analysis. Next, we demonstrated that AREG enhances
81 reprogramming both *in vitro* and *in vivo* via EGFR and alleviates the age-associated reduction in
82 reprogramming.
83
84 **RESULTS**
85 **Paracrine senescence promotes *in vitro* reprogramming in a stress-dependent manner**
86 Given senescence can impact reprogramming in both cell-autonomous and non-cell-autonomous
87 manner (Chiche et al., 2020), and SASP composition is highly context-dependent, determined by both
88 the initial stress and the tissue/cell of origin(Hernandez-Segura et al., 2017; Ito et al., 2017). We
89 reasoned stress dependent SASP might impact reprogramming efficiency differently. To address this
90 question, we treated non-reprogrammable wild-type (WT) primary mouse embryonic fibroblasts
91 (MEFs) with three different stimuli (replicative senescence (RS), γ-irradiation (IRIS), and oncogene-
92 induced senescence (OIS)) to induce senescence and generate distinct SASP (Figure S1A). Meanwhile,
93 we used the MEFs generated from a previously established reprogrammable mouse model (i4F) (Abad
94 et al., 2013). The reprogramming was induced by adding doxycycline (DOX) in i4F-MEFs either co-
95 cultured with the senescent WT MEFs (co-culture) or cultured directly with the senescence
96 conditioned medium (CM) according to the experimental scheme illustrated (Figure 1A). After 12
97 days DOX treatment, induced pluripotent stem cells (iPSCs) colonies were stained using alkaline
98 phosphatase (AP) to determine the reprogramming efficiency. For the co-culture system, i4F MEFs
99 were seeded on top of $2x10^5$ WT MEFs (either control or OIS treated) with various ratios of 1:3, 1:5,
100 and 1:10 (i4F: WT), to determine the optimal experimental condition. We found the reprogramming
101 efficiency increased the most in the ratio of 1:10 (i4F: WT) (Figure S1B). Next, we compared the
102 relative reprogramming efficiency of i4F MEFs and found that in both systems all stimuli can increase
103 reprogramming efficiency ranging from RS the least to OIS the most, except the positive effect of RS
104 is diminished in the CM system (Figure 1B & Figure 1C).
105
106 Reprogramming is a stepwise process with distinct phases: initiation, maturation, and stabilization
107 (Samavarchi-Tehrani et al., 2010). To determine at which stage the SASP exposure is most important
108 for enhancing reprogramming, we cultured i4F with either OIS-CM or Ctrl-CM in different order
109 (Figure 1D & Figure S1C). Culturing i4F-MEFs with OIS-CM for the first three days was sufficient to
110 induce the highest fold increase in reprogramming (Figure 1D). Conversely, initiating reprogramming
111 with Ctrl-CM for three days and replaced by OIS-CM completely abolished the beneficial effect

112 (Figure S1C). Active cell proliferation is rate-limiting for successful reprogramming (Ruiz et al.,
113 2011), and senescent cells secrete various growth factors (Coppe et al., 2010). Therefore, we
114 compared the growth properties of i4F MEFs cultured with either OIS-CM or Ctrl-CM over 12 days in
115 the absence of DOX. The bromodeoxyuridine (BrdU) incorporation rates after 72 hours were similar
116 between Ctrl and OIS (Figure S1E). However, the accumulative growth curve indicated that i4F MEFs
117 grew faster in OIS-CM than in Ctrl-CM (Figure S1D). Hence, certain SASP factors promote *in vitro*
118 reprogramming transiently at the initiation phase of reprogramming, which partially correlates with an
119 enhanced proliferation rate.
120
121 **Conditioned medium of OIS-Il6$^{-/-}$ promoted reprogramming efficiently**
122 We sought to identify SASP factors responsible for the stress-dependent effect on reprogramming.
123 Given that IL-6 signaling is required for *in vitro* reprogramming (Brady et al., 2013; Mai et al., 2018),
124 and IL-6 is a crucial mediator of the senescence paracrine signals in promoting *in vivo* reprogramming
125 (Chiche et al., 2017; Mosteiro et al., 2016; Mosteiro et al., 2018), we determined firstly the effect of
126 CM of senescent MEFs derived from *Il6*$^{-/-}$ mice on reprogramming. Of note, IL-6 plays a critical role
127 in mediating OIS, and reduction of IL-6 via RNA interference efficiently bypassed OIS in human
128 diploid fibroblasts (Kuilman et al., 2008). Interestingly, we found *Il6*$^{-/-}$ MEF entered senescence
129 efficiently upon OIS, judging by both senescence-associated beta-galactosidase (SAβGal) staining
130 (data not shown) and qPCR (Figure S2A). Surprisingly, CM generated from senescent *Il6*$^{-/-}$ MEFs by
131 IRIS or OIS enhanced reprogramming efficiency to a similar level as WT (Figure 2A). To ensure the
132 observed enhancement is IL-6 independent, we compared the IL-6 level in the OIS-CMs of both WT
133 and *Il6*$^{-/-}$ by ELISA. In WT, IL-6 is significantly increased in the OIS-CM compared to Ctrl-CM.
134 While, IL-6 is non-detectable in both Ctrl-CM and OIS-CM of *Il6*$^{-/-}$ (Figure S2B). Of note, IL-6
135 neutralizing antibody could potently repress the increased reprogramming efficiency only in the CM-
136 WT but failed to do so in the CM-*Il6*$^{-/-}$ (Figure 2B and Figure S2C). Thus, there are SASP factors
137 other than IL-6 that can robustly promote *in vitro* reprogramming.
138
139 ***In vivo* reprogramming in the skeletal muscle is not affected by IL6 deficiency**
140 We reported previously that injury-induced senescence enabled reprogramming in the skeletal muscle
141 (Chiche et al., 2017). We wondered whether tissue injury could induce reprogramming in the skeletal
142 muscle of *Il6*$^{-/-}$ mice. To test this, we generated *Il6*$^{-/-}$;i4F mouse model and injured the Tibialis anterior
143 (TA) muscle of both *Il6*$^{+/-}$;i4F and *Il6*$^{-/-}$;i4F mice with the snake venom cardiotoxin (CTX). In the
144 same time, we added doxycycline (dox) in the drinking water for 7 days to induce *in vivo*
145 reprogramming and TAs were collected at 10 days post-injury (DPI) as previously described (Chiche
146 et al., 2017). The expression of the OSKM triggered extensive dysplasia and reprogramming (Nanog^{+}
147 cells) in the injured TA of male i4F mice (Figure 2C and Figure S2D). Consistent with a previous
148 report (Mosteiro et al., 2018), the reprogramming was significantly reduced in the females i4F mice

149 comparing to male i4F mice (Figure 2C & 2D,0 Figure S2D). Interestingly, *Il6*$^{-/-}$; i4F mice exhibited a
150 similar level of dysplasia and Nanog^{+} cells as the sex-matched *Il6*$^{+/-}$;i4F mice (Figure 2C & 2D, Figure
151 S2D). Besides, we did not observe a difference in the senescence induction in males regardless of the
152 genotype (Figure S2E & S2F). Thus, *in vivo* reprogramming in the skeletal muscle is not impaired in
153 the IL-6 deficient reprogrammable mice.
154
155 **Soluble factor fraction of the CM-OIS mediates *in vitro* reprogramming**
156 To gain a comprehensive profile of the SASP heterogenous composition, we determined firstly the
157 effect of different fractions of CM on reprogramming, which could facilitate reprogramming due to
158 secreted proteins, extracellular vesicles, or small-molecule metabolites. We examined whether the
159 boiled CM could promote *in vitro* reprogramming since boiling denatures most proteins without
160 affecting small molecule metabolites, and found that boiled CM completely abolished *in vitro*
161 reprogramming, indicating that secreted proteins are crucial in promoting reprogramming (Figure
162 S3A).
163
164 Exosomes are small extracellular vesicles (sEV) released from almost all cell types and are critical
165 mediators of intercellular communication (Kalluri and LeBleu, 2020). Increasing evidence suggests
166 that senescent cells secret exosomes with distinct features, contributing to paracrine senescence
167 (Borghesan et al., 2019). To examine whether senescence-associated exosomes regulate *in vitro*
168 reprogramming, we isolated sEV and supernatants (SN) fractions from Ctrl-CM and OIS-CM using
169 serial ultracentrifugation and filtering with a 0.22-µm filter (Thery et al., 2006). Both OIS-sEV and
170 Ctrl-sEV were suspended in Ctrl-SN to determine whether they can drive paracrine senescence.
171 Consistent with the previous report (Borghesan et al., 2019), the OIS-sEV in Ctrl-SN induces several
172 senescence markers in i4F MEFs, as shown by a decrease in BrdU incorporation and an increase in
173 mRNA expression of p16 and ARF (Figure S3B & Figure S3C). Next, we wondered whether OIS-sEV
174 could also affect reprogramming. Comparing to Ctrl-SN, the OIS-SN significantly enhanced the
175 reprogramming efficiency to a similar level as OIS-CM (Figure 3A). However, OIS-sEV in Ctrl-SN
176 exhibited a much lower reprogramming efficiency than OIS-SN, similarly to Ctrl-sEV in Ctrl-SN
177 (Figure 3A). Hence, the soluble fraction of OIS-CM is essential for promoting in vitro reprogramming.
178
179 **Quantitative proteomics analysis of SASP composition**
180 To gain a comprehensive profile of the heterogenous SASP composition and maximize the detection
181 of SASP factors important for reprogramming other than IL6, we isolated the soluble protein fractions
182 from the OIS-CM and Ctrl-CM of *Il6*$^{-/-}$ MEFs to perform quantitative proteomic analysis. The label-
183 free data-independent acquisition (DIA) tandem mass spectrometry strategy allows sensitive and
184 unbiased detection of SASP proteins in a reproducible manner (Basisty et al., 2020; Gillet et al., 2012).
185 To ensure the correct identification, we only included a protein when it can be detected in all six

186 replicates of one condition. The proteomic analysis identified a total of 1955 proteins in both
187 conditions, including 249 proteins with a significant differential expression (q-value <0.01) that had a
188 fold change of at least 2-fold (SEN/CTL) (Figure 3B). Of note, 217 proteins were exclusively detected
189 in one condition (185 in SEN and 32 in CTL) (Figure 3C), which were assumed differentially
190 abundant between the conditions and included in the data analysis. We found many known SASP
191 factors are more abundantly secreted in the OIS-SN, such as SPP1, PLAU, and MMP3 (Figure S3D).
192 Of note, we did not detect IL-6 in both conditions. Interestingly, there is less than 50% overlap
193 between our study and a recent large-scale human SASP proteomic study (human fibroblast-OIS,
194 115/386), suggesting heterogenous in SASP composition between species (Hernandez-Segura et al.,
195 2017).
196
197 To identify which biological pathways/responses are mediated by SASP factors, we performed
198 pathway and network analyses on the proteins that are either more abundantly or exclusively secreted
199 from the SEN condition. We found the most dominant clusters of gene ontology (GO) pathways are
200 related to morphogenesis and stress response, including cell morphogenesis in development and
201 differentiation, response to growth factor, wounding response, and angiogenesis (Figure 3D). Besides,
202 the hallmark gene set enrichment analysis (GSEA) revealed several pathways that are associated with
203 paracrine senescence, including Epithelial-to-Mesenchymal transition (EMT) (Ansieau et al., 2008),
204 TNFα signaling via NFκB, inflammatory response, and p53 pathway (Coppe et al., 2010) (Figure
205 S3E).
206
207 **Amphiregulin enhances *in vitro* reprogramming efficiency and kinetic**
208 Of note, several pathways identified by the bioinformatic analysis are also important for somatic
209 reprogramming, such as EMT (Liu et al., 2013), apoptosis (Kawamura et al., 2009; Kim et al., 2018),
210 hypoxia (Yoshida et al., 2009), and p53 pathway (Hong et al., 2009; Kawamura et al., 2009; Marion et
211 al., 2009; Utikal et al., 2009). Given Mesenchymal-to-Epithelial transition (MET) is required in the
212 initiation phase of *in vitro* reprogramming (Li et al., 2010; Liu et al., 2013; Samavarchi-Tehrani et al.,
213 2010), and because our data suggested that paracrine senescence promotes reprogramming at the early
214 stage (Figure 1D), we investigated the proteins overlapped with the EMT gene set and found many
215 factors crucial for *in vitro* reprogramming, such as BMP1 and TGFβ (Li et al., 2010; Liu et al., 2013;
216 Samavarchi-Tehrani et al., 2010)(Figure S4A).
217
218 AREG is an EGFR ligand (Shoyab et al., 1989) and has diverse functions in development, tissue
219 regeneration, and tumorigenesis (Zaiss et al., 2015). Since both OIS and muscle injury strongly induce
220 AREG (Burzyn et al., 2013; Pommer et al., 2021), we wondered whether AREG could partially
221 mediate the effect of paracrine senescence on reprogramming both *in vitro* and *in vivo*. Interestingly,

222 AREG is the only EGFR ligand that has significantly increased mRNA expression in OIS comparing
223 to IRIS (Figure S4B). To formally test the effect of AREG on reprogramming, we added different
224 concentrations of the recombinant AREG protein for the first three days during reprogramming,
225 consistent with the CM experiment (Figure 1D). AREG treatment enhanced reprogramming efficiency
226 in a dosage-dependent manner (Figure 4A). We next removed DOX at different time points to
227 examine the ability of AREG to facilitate OSKM transgene-independent clonal growth, a hallmark of
228 iPSCs. AREG treatment yielded iPSCs clones after only 5 days of OSKM expression, compared to 8
229 days in the control condition (Figure 4B), suggesting a faster reprogramming kinetic.
230
231 **AREG accelerates cell cycle and the process of MET during reprogramming**
232 We sought to understand the mechanism by which AREG promotes reprogramming. The reported role
233 of AREG in proliferation and EMT (Berasain and Avila, 2014) prompted us to analyze cell
234 proliferation and MET process, two vital cellular events that occurred in the early stage of
235 reprogramming (Sancho-Martinez and Izpisua Belmonte, 2013). We found that AREG treatment led to
236 a larger fraction of cells in S-phase and increased cell proliferation globally in MEFs alone (Figure
237 S4C & S4D). Next, we checked whether AREG affected MET during reprogramming by measuring
238 the expression of several mesenchymal and epithelial cell markers at different time points throughout
239 reprogramming using qPCR. In control, the expression of the mesenchymal markers, Zeb1 and Zeb2,
240 were transiently upregulated and gradually suppressed afterward. Interestingly, these markers were
241 suppressed throughout the reprogramming process in AREG treated condition (Figure 4C). Conversely,
242 the expression of the epithelial markers, Occludin and E-Cadherin, was higher in samples treated with
243 AREG than the control (Figure 4D). Besides, the expression of all the pluripotency markers,
244 endogenous Oct4, Sox2, Klf4, Nanog, Lin28, and Esrrb, gradually increased and peaked at the last
245 stage reprogramming in control. While in AREG treated condition, endogenous Oct4 and Nanog
246 expression sharply increased at 6 days and reached the plateau earlier than in the control (Figure 4E).
247 However, the expression dynamic of other pluripotent markers remained the same (Figure S4D),
248 suggesting an action upon Nanog and Oct4 specifically rather than a mere reflection of the accelerated
249 reprogramming. Taken together, these results indicate that AREG enhances the efficiency and kinetic
250 of reprogramming by increasing proliferation rates and facilitating MET process.
251
252 **EGFR signaling pathway is important for reprogramming**
253 Since AREG is an atypical EGFR ligand (Zaiss et al., 2015), we wondered whether other EGFR
254 ligands could also promote somatic reprogramming and found that additional epidermal growth factor
255 (EGF) also improved the reprogramming efficiency (Figure 5A). Next, we examined whether EGFR
256 activation is necessary for the enhancement. AREG and Dox combination strongly induced the
257 activation of EGFR comparing to Dox alone or untreated control determined by the level of the
258 phosphorylated EGFR using Western blotting (Figure S5A). Besides, Lapatinib, a dual tyrosine kinase

259 inhibitor of EGFR and human epidermal growth factor receptor-2 (HER2) (Wood et al., 2004),
260 canceled the effect of AREG on reprogramming (Figure 5B and Figure S5A). Of note, a high
261 concentration of Lapatinib alone significantly repressed reprogramming (Figure S5B), suggesting
262 EGFR signaling pathway might be required for reprogramming. Hence, AREG promotes
263 reprogramming in an EGFR dependent manner.
264
265 **AREG rescues age-dependent reduction in reprogramming**
266 Previously, we reported that murine dermal fibroblasts (MDFs) derived from old (> 2 years) mice had
267 a significant reduction in reprogramming efficiency comparing to MDFs derived from young (2
268 months) mice (Li et al., 2009). Because AREG induces cell proliferation, we investigated whether
269 AREG can improve reprogramming in this context. Consistent with the previous report, MDFs from
270 old (> 2 years) i4F mice had much lower reprogramming efficiency comparing to MDFs from young
271 (2 months) i4F mice (Figure 5C). Notably, the addition of AREG to the aged MDFs rescued their low
272 reprogramming efficiency to the same level as the young MDFs (Figure 5C).
273
274 **AREG promotes *in vivo* reprogramming in the skeletal muscle**
275 It has been reported that AREG enhances the myogenic differentiation of skeletal muscle stem cells
276 (MuSCs) *in vitro* and facilitates muscle regeneration (Burzyn et al., 2013). We previously reported
277 that MuSC is a cell of origin for *in vivo* reprogramming (Chiche et al., 2017). Therefore, we
278 hypothesize that AREG might also improve *in vivo* reprogramming in the injured muscle. To address
279 this question, we administered AREG to the CTX-injured, DOX-treated male i4F mice according to
280 the experimental scheme illustrated in Figure 5D and evaluated reprogramming and senescence
281 induction at 10 DPI. (Note that the initial AREG injection was done i.m. as previously described
282 (Burzyn et al., 2013).) There were many more Nanog+ cells in the TA sections from mice treated with
283 AREG comparing to the control group (Figure 5E and Figure 5F). Conversely, there is no apparent
284 difference in senescence induction, detected by SAβGal staining (Figure 5E and Figure 5F). Because
285 AREG was administrated mainly i.p., we wondered whether it could also improve reprogramming in
286 other tissues. Interestingly, we also observed more Nanog+ cells in both pancreas and kidney, but not
287 in the liver (Figure S5C), suggesting a tissue-specific effect of AREG on *in vivo* reprogramming.
288
289 **Discussion:**
290 Here, we report that the impact of paracrine senescence on reprogramming is stress-dependent. The
291 quantitative proteomic analysis on the senescence-associated secretome identified a catalog of factors
292 involved in various biological processes that could potentially impact cell plasticity. We demonstrated
293 that the AREG enhances *in vitro* reprogramming efficiency and kinetic, at least in part, by accelerating
294 somatic cell proliferation and the process of MET. Of note, AREG treatment rescue the age-associated
295 reduction in reprogramming and facilitate *in vivo* reprogramming in a tissue-specific manner.

296
297 IL-6 is required for oncogene-induced senescence (Kuilman et al., 2008). Surprisingly, we could
298 efficiently induce senescence in *Il6*$^{-/-}$ MEFs (Figure S2A)(Kopf et al., 1994). Both ELISA and
299 proteomic analysis failed to detect IL-6 in the CM-OIS-*Il6*$^{-/-}$ (Figure S2B and Figure S2C), indicating
300 that OIS-*Il6*$^{-/-}$ does not secrete IL-6. Thus, the discrepancy might be due to the compensation effect of
301 germline knockout, which often yields much weaker phenotypes than acute disruption of gene
302 function (Housden et al., 2017). Importantly, IL-6 blocking antibody did not abolish the beneficial
303 effect of CM-OIS-*Il6*$^{-/-}$ on *in vitro* reprogramming (Figure 2B), highlighting the involvement of other
304 SASP factors.
305
306 Consistently, we found that IL-6 deficiency supports *in vivo* reprogramming in the muscle (Figure 2C
307 and Figure 2D). Together with others, we have previously demonstrated that tissue injury-induced
308 senescence facilitates *in vivo* reprogramming in a paracrine manner, particularly by IL-6 (Chiche et al.,
309 2017; Mosteiro et al., 2016). A recent study reported a reduction of reprogramming in the pancreas of
310 i4F; *Il6*$^{-/-}$ mice (Mosteiro et al., 2018). Firstly, reprogramming-induced and injury-induced senescence
311 might produce different factors (Chiche et al., 2017; Mosteiro et al., 2018). Besides, IL-6 is a myokine
312 vital for muscle formation and growth (Serrano et al., 2008). Although many different cell types
313 produce IL-6 upon muscle injury, including macrophages and muscle stem cells (Munoz-Canoves et
314 al., 2013), muscle regeneration is only mildly affected in *Il6*$^{-/-}$ mice (Zhang et al., 2013), suggesting a
315 potential compensation by other members of the IL-6 cytokine family. Therefore, the tissue-specific
316 requirement of IL-6 for *in vivo* reprogramming might be due to distinct stress/tissue-dependent
317 senescence secretome and the pleiotropic functions of IL-6.
318
319 To gain an extensive and quantitative view on SASP factors, we performed an unbiased proteomic
320 study using CM-OIS-*Il6*$^{-/-}$ (Figure 3B). The bioinformatic network analysis revealed pathways
321 predominantly related to morphogenesis and response to growth factors (Figure 3C), where EGFR
322 signaling pathways play crucial roles. Of note, we used OIS-MEFs as a proxy for senescence induced
323 by OSKM over-expression or muscle injury to identify SASP factors, which might not fully
324 recapitulate the *in vivo* scenario. Future investigation will further elucidate the context-dependent
325 SASP heterogeneity.
326
327 To shed some light on SASP factors other than IL-6 and reprogramming, we investigated the role of
328 AREG in this process. We found that AREG treatment could notably increase *in vitro* reprogramming
329 efficiency (Figure 4A) and kinetic (Figure 4B). Next, we showed that AREG could accelerate cell
330 proliferation (Figure S4C) and suppress mesenchymal markers (Figure 4C), suggesting AREG might
331 affect several cellular events necessary for the initiation phase of reprogramming(Sancho-Martinez
332 and Izpisua Belmonte, 2013). Interestingly, we found AREG could alleviate the negative impact of

333 age on reprogramming (Figure 5B), providing a straightforward solution to improve iPS cell
334 generation during aging (Mahmoudi et al., 2019). Of note, AREG treatment failed to further enhance
335 reprogramming to the similar level as the young (Figure 5B), reflecting the attenuated EGFR signaling
336 in the aged skin fibroblasts as previously reported (Shiraha et al., 2000; Tran et al., 2003).
337
338 Furthermore, we showed that AREG promotes *in vivo* reprogramming in the muscle (Figure 5E & 5F).
339 It has been reported that EGFR regulates the asymmetrical division of MuSCs (Wang et al., 2019), and
340 AREG could facilitate the differentiation of MuSCs *in vitro* (Burzyn et al., 2013; Zaiss et al., 2015).
341 Therefore, AREG might directly promote the cell plasticity of MuSCs, a primary cell origin of
342 reprogramming in the muscle (Chiche et al., 2017). Interestingly, AREG also promoted
343 reprogramming in the pancreas and kidney but not in the liver (Figure S5C), highlighting a tissue-
344 specific mode of action. Of note, recent studies showed that cyclic expression of OSKM could
345 enhance muscle regeneration (Ocampo et al., 2016). Given senescence is important for optimal wound
346 healing (Demaria et al., 2014) and limb regeneration (Yun et al., 2015), future investigation is
347 warranted to determine whether the rejuvenation effect of partial reprogramming is partially mediated
348 by senescence.
349
350 In summary, we dissected the impact of paracrine senescence on reprogramming and revealed the role
351 of the AREG-EGFR signaling pathway in reprogramming. These findings may have important
352 implications for understanding senescence's involvement in tissue repair and *in vivo* reprogramming.

Acknowledgements

We are indebted to Jun Zhang for his excellent technical support in image analysis. We are grateful to the Central Animal Facility, the Proteomic Platform, the Cytometry Platform, and the Bioinformatics and Biostatistics Hub of the Institut Pasteur. Work in the laboratory of H.L. was funded by Institut Pasteur, Centre National pour la Recherche Scientific and the Agence Nationale de la Recherche (Laboratoire d'Excellence Revive, Investissement d'Avenir; ANR-10-LABX- 73; ANR-16-CE13-0017). This work is also supported by Fondation ARC (PJA 20161205028). AC was funded by the postdoctoral fellowships from the Revive Consortium.

AUTHOR CONTRIBUTIONS

M.VJ performed most of the experimental work, contributed to experimental design, data analysis, and discussions. C.C made critical experimental contributions. AC contributed experimentally. T.D performed proteomic analysis and data acquisition. M.M supervised the proteomic analysis and data interpretation. H.L. supervised the study, designed the experimental plan, interpreted the data and wrote the manuscript. All authors discussed the results and commented on the manuscript. The authors declare no competing financial interests with this paper.

REFERENCE

Aarts, M., Georgilis, A., Beniazza, M., Beolchi, P., Banito, A., Carroll, T., Kulisic, M., Kaemena, D.F., Dharmalingam, G., Martin, N., *et al*. (2017). Coupling shRNA screens with single-cell RNA-seq identifies a dual role for mTOR in reprogramming-induced senescence. Genes Dev *31*, 2085-2098.

Ansieau, S., Bastid, J., Doreau, A., Morel, A.P., Bouchet, B.P., Thomas, C., Fauvet, F., Puisieux, I., Doglioni, C., Piccinin, S., *et al*. (2008). Induction of EMT by twist proteins as a collateral effect of tumor-promoting inactivation of premature senescence. Cancer Cell *14*, 79-89.

Banito, A., Rashid, S.T., Acosta, J.C., Li, S., Pereira, C.F., Geti, I., Pinho, S., Silva, J.C., Azuara, V., Walsh, M., *et al*. (2009). Senescence impairs successful reprogramming to pluripotent stem cells. Genes Dev *23*, 2134-2139.

Basisty, N., Kale, A., Jeon, O.H., Kuehnemann, C., Payne, T., Rao, C., Holtz, A., Shah, S., Sharma, V., Ferrucci, L., *et al*. (2020). A proteomic atlas of senescence-associated secretomes for aging biomarker development. PLoS Biol *18*, e3000599.

Berasain, C., and Avila, M.A. (2014). Amphiregulin. Semin Cell Dev Biol *28*, 31-41.

Bindea, G., Mlecnik, B., Hackl, H., Charoentong, P., Tosolini, M., Kirilovsky, A., Fridman, W.H., Pages, F., Trajanoski, Z., and Galon, J. (2009). ClueGO: a Cytoscape plug-in to decipher functionally grouped gene ontology and pathway annotation networks. Bioinformatics *25*, 1091-1093.

Borghesan, M., Fafian-Labora, J., Eleftheriadou, O., Carpintero-Fernandez, P., Paez-Ribes, M., Vizcay-Barrena, G., Swisa, A., Kolodkin-Gal, D., Ximenez-Embun, P., Lowe, R., *et al*. (2019). Small

Extracellular Vesicles Are Key Regulators of Non-cell Autonomous Intercellular Communication in Senescence via the Interferon Protein IFITM3. Cell Rep *27*, 3956-3971 e3956.
Brady, J.J., Li, M., Suthram, S., Jiang, H., Wong, W.H., and Blau, H.M. (2013). Early role for IL-6 signalling during generation of induced pluripotent stem cells revealed by heterokaryon RNA-Seq. Nat Cell Biol *15*, 1244-1252.
Burzyn, D., Kuswanto, W., Kolodin, D., Shadrach, J.L., Cerletti, M., Jang, Y., Sefik, E., Tan, T.G., Wagers, A.J., Benoist, C., *et al*. (2013). A special population of regulatory T cells potentiates muscle repair. Cell *155*, 1282-1295.
Chiche, A., Chen, C., and Li, H. (2020). The crosstalk between cellular reprogramming and senescence in aging and regeneration. Exp Gerontol *138*, 111005.
Chiche, A., Le Roux, I., von Joest, M., Sakai, H., Aguin, S.B., Cazin, C., Salam, R., Fiette, L., Alegria, O., Flamant, P., *et al*. (2017). Injury-Induced Senescence Enables In Vivo Reprogramming in Skeletal Muscle. Cell Stem Cell *20*, 407-414 e404.
Coppe, J.P., Desprez, P.Y., Krtolica, A., and Campisi, J. (2010). The senescence-associated secretory phenotype: the dark side of tumor suppression. Annu Rev Pathol *5*, 99-118.
Demaria, M., Ohtani, N., Youssef, S.A., Rodier, F., Toussaint, W., Mitchell, J.R., Laberge, R.M., Vijg, J., Van Steeg, H., Dolle, M.E., *et al*. (2014). An essential role for senescent cells in optimal wound healing through secretion of PDGF-AA. Dev Cell *31*, 722-733.
Gillet, L.C., Navarro, P., Tate, S., Rost, H., Selevsek, N., Reiter, L., Bonner, R., and Aebersold, R. (2012). Targeted data extraction of the MS/MS spectra generated by data-independent acquisition: a new concept for consistent and accurate proteome analysis. Mol Cell Proteomics *11*, O111 016717.
Herbst, R.S. (2004). Review of epidermal growth factor receptor biology. Int J Radiat Oncol Biol Phys *59*, 21-26.
Hernandez-Segura, A., de Jong, T.V., Melov, S., Guryev, V., Campisi, J., and Demaria, M. (2017). Unmasking Transcriptional Heterogeneity in Senescent Cells. Curr Biol *27*, 2652-2660 e2654.
Hernandez-Segura, A., Nehme, J., and Demaria, M. (2018). Hallmarks of Cellular Senescence. Trends Cell Biol *28*, 436-453.
Hong, H., Takahashi, K., Ichisaka, T., Aoi, T., Kanagawa, O., Nakagawa, M., Okita, K., and Yamanaka, S. (2009). Suppression of induced pluripotent stem cell generation by the p53-p21 pathway. Nature *460*, 1132-1135.
Housden, B.E., Muhar, M., Gemberling, M., Gersbach, C.A., Stainier, D.Y., Seydoux, G., Mohr, S.E., Zuber, J., and Perrimon, N. (2017). Loss-of-function genetic tools for animal models: cross-species and cross-platform differences. Nat Rev Genet *18*, 24-40.
Ito, Y., Hoare, M., and Narita, M. (2017). Spatial and Temporal Control of Senescence. Trends Cell Biol *27*, 820-832.
Jones, J.T., Akita, R.W., and Sliwkowski, M.X. (1999). Binding specificities and affinities of egf domains for ErbB receptors. FEBS Lett *447*, 227-231.
Kalluri, R., and LeBleu, V.S. (2020). The biology, function, and biomedical applications of exosomes. Science *367*.
Kawamura, T., Suzuki, J., Wang, Y.V., Menendez, S., Morera, L.B., Raya, A., Wahl, G.M., and Belmonte, J.C. (2009). Linking the p53 tumour suppressor pathway to somatic cell reprogramming. Nature *460*, 1140-1144.
Kim, C.H., Chae, H.D., Cheon, Y.P., Kang, B.M., Chang, Y.S., and Mok, J.E. (1999). The effect of epidermal growth factor on the preimplantation development, implantation and its receptor expression in mouse embryos. J Obstet Gynaecol Res *25*, 87-93.
Kim, E.J.Y., Anko, M.L., Flensberg, C., Majewski, I.J., Geng, F.S., Firas, J., Huang, D.C.S., van Delft, M.F., and Heath, J.K. (2018). BAK/BAX-Mediated Apoptosis Is a Myc-Induced Roadblock to Reprogramming. Stem Cell Reports *10*, 331-338.
Kopf, M., Baumann, H., Freer, G., Freudenberg, M., Lamers, M., Kishimoto, T., Zinkernagel, R., Bluethmann, H., and Kohler, G. (1994). Impaired immune and acute-phase responses in interleukin-6-deficient mice. Nature *368*, 339-342.
Kuilman, T., Michaloglou, C., Vredeveld, L.C., Douma, S., van Doorn, R., Desmet, C.J., Aarden, L.A., Mooi, W.J., and Peeper, D.S. (2008). Oncogene-induced senescence relayed by an interleukin-dependent inflammatory network. Cell *133*, 1019-1031.

Li, H., Collado, M., Villasante, A., Strati, K., Ortega, S., Canamero, M., Blasco, M.A., and Serrano, M. (2009). The Ink4/Arf locus is a barrier for iPS cell reprogramming. Nature *460*, 1136-1139.
Li, R., Liang, J., Ni, S., Zhou, T., Qing, X., Li, H., He, W., Chen, J., Li, F., Zhuang, Q., *et al*. (2010). A mesenchymal-to-epithelial transition initiates and is required for the nuclear reprogramming of mouse fibroblasts. Cell Stem Cell *7*, 51-63.
Liu, X., Sun, H., Qi, J., Wang, L., He, S., Liu, J., Feng, C., Chen, C., Li, W., Guo, Y., *et al*. (2013). Sequential introduction of reprogramming factors reveals a time-sensitive requirement for individual factors and a sequential EMT-MET mechanism for optimal reprogramming. Nat Cell Biol *15*, 829-838.
Mahmoudi, S., Mancini, E., Xu, L., Moore, A., Jahanbani, F., Hebestreit, K., Srinivasan, R., Li, X., Devarajan, K., Prelot, L., *et al*. (2019). Heterogeneity in old fibroblasts is linked to variability in reprogramming and wound healing. Nature *574*, 553-558.
Mai, T., Markov, G.J., Brady, J.J., Palla, A., Zeng, H., Sebastiano, V., and Blau, H.M. (2018). NKX3-1 is required for induced pluripotent stem cell reprogramming and can replace OCT4 in mouse and human iPSC induction. Nat Cell Biol *20*, 900-908.
Marion, R.M., Strati, K., Li, H., Tejera, A., Schoeftner, S., Ortega, S., Serrano, M., and Blasco, M.A. (2009). Telomeres acquire embryonic stem cell characteristics in induced pluripotent stem cells. Cell Stem Cell *4*, 141-154.
Mosteiro, L., Pantoja, C., Alcazar, N., Marion, R.M., Chondronasiou, D., Rovira, M., Fernandez-Marcos, P.J., Munoz-Martin, M., Blanco-Aparicio, C., Pastor, J., *et al*. (2016). Tissue damage and senescence provide critical signals for cellular reprogramming in vivo. Science *354*.
Mosteiro, L., Pantoja, C., de Martino, A., and Serrano, M. (2018). Senescence promotes in vivo reprogramming through p16(INK)(4a) and IL-6. Aging Cell *17*.
Munoz-Canoves, P., Scheele, C., Pedersen, B.K., and Serrano, A.L. (2013). Interleukin-6 myokine signaling in skeletal muscle: a double-edged sword? FEBS J *280*, 4131-4148.
Munoz-Espin, D., and Serrano, M. (2014). Cellular senescence: from physiology to pathology. Nat Rev Mol Cell Biol *15*, 482-496.
Ocampo, A., Reddy, P., Martinez-Redondo, P., Platero-Luengo, A., Hatanaka, F., Hishida, T., Li, M., Lam, D., Kurita, M., Beyret, E., *et al*. (2016). In Vivo Amelioration of Age-Associated Hallmarks by Partial Reprogramming. Cell *167*, 1719-1733 e1712.
Pommer, M., Kuphal, S., and Bosserhoff, A.K. (2021). Amphiregulin Regulates Melanocytic Senescence. Cells *10*.
Rhinn, M., Ritschka, B., and Keyes, W.M. (2019). Cellular senescence in development, regeneration and disease. Development *146*.
Ruiz, S., Panopoulos, A.D., Herrerias, A., Bissig, K.D., Lutz, M., Berggren, W.T., Verma, I.M., and Izpisua Belmonte, J.C. (2011). A high proliferation rate is required for cell reprogramming and maintenance of human embryonic stem cell identity. Curr Biol *21*, 45-52.
Samavarchi-Tehrani, P., Golipour, A., David, L., Sung, H.K., Beyer, T.A., Datti, A., Woltjen, K., Nagy, A., and Wrana, J.L. (2010). Functional genomics reveals a BMP-driven mesenchymal-to-epithelial transition in the initiation of somatic cell reprogramming. Cell Stem Cell *7*, 64-77.
Sancho-Martinez, I., and Izpisua Belmonte, J.C. (2013). Stem cells: Surf the waves of reprogramming. Nature *493*, 310-311.
Schuldiner, M., Yanuka, O., Itskovitz-Eldor, J., Melton, D.A., and Benvenisty, N. (2000). Effects of eight growth factors on the differentiation of cells derived from human embryonic stem cells. Proc Natl Acad Sci U S A *97*, 11307-11312.
Serrano, A.L., Baeza-Raja, B., Perdiguero, E., Jardi, M., and Munoz-Canoves, P. (2008). Interleukin-6 is an essential regulator of satellite cell-mediated skeletal muscle hypertrophy. Cell Metab *7*, 33-44.
Shiraha, H., Gupta, K., Drabik, K., and Wells, A. (2000). Aging fibroblasts present reduced epidermal growth factor (EGF) responsiveness due to preferential loss of EGF receptors. J Biol Chem *275*, 19343-19351.
Shoyab, M., McDonald, V.L., Bradley, J.G., and Todaro, G.J. (1988). Amphiregulin: a bifunctional growth-modulating glycoprotein produced by the phorbol 12-myristate 13-acetate-treated human breast adenocarcinoma cell line MCF-7. Proc Natl Acad Sci U S A *85*, 6528-6532.
Shoyab, M., Plowman, G.D., McDonald, V.L., Bradley, J.G., and Todaro, G.J. (1989). Structure and function of human amphiregulin: a member of the epidermal growth factor family. Science *243*, 1074-1076.

Thery, C., Amigorena, S., Raposo, G., and Clayton, A. (2006). Isolation and characterization of exosomes from cell culture supernatants and biological fluids. Curr Protoc Cell Biol *Chapter 3*, Unit 3 22.
Tran, K.T., Rusu, S.D., Satish, L., and Wells, A. (2003). Aging-related attenuation of EGF receptor signaling is mediated in part by increased protein tyrosine phosphatase activity. Exp Cell Res *289*, 359-367.
Utikal, J., Polo, J.M., Stadtfeld, M., Maherali, N., Kulalert, W., Walsh, R.M., Khalil, A., Rheinwald, J.G., and Hochedlinger, K. (2009). Immortalization eliminates a roadblock during cellular reprogramming into iPS cells. Nature *460*, 1145-1148.
Wang, Y.X., Feige, P., Brun, C.E., Hekmatnejad, B., Dumont, N.A., Renaud, J.M., Faulkes, S., Guindon, D.E., and Rudnicki, M.A. (2019). EGFR-Aurka Signaling Rescues Polarity and Regeneration Defects in Dystrophin-Deficient Muscle Stem Cells by Increasing Asymmetric Divisions. Cell Stem Cell *24*, 419-432 e416.
Wood, E.R., Truesdale, A.T., McDonald, O.B., Yuan, D., Hassell, A., Dickerson, S.H., Ellis, B., Pennisi, C., Horne, E., Lackey, K., *et al*. (2004). A unique structure for epidermal growth factor receptor bound to GW572016 (Lapatinib): relationships among protein conformation, inhibitor off-rate, and receptor activity in tumor cells. Cancer Res *64*, 6652-6659.
Xu, Q., Long, Q., Zhu, D., Fu, D., Zhang, B., Han, L., Qian, M., Guo, J., Xu, J., Cao, L., *et al*. (2019). Targeting amphiregulin (AREG) derived from senescent stromal cells diminishes cancer resistance and averts programmed cell death 1 ligand (PD-L1)-mediated immunosuppression. Aging Cell *18*, e13027.
Yoshida, Y., Takahashi, K., Okita, K., Ichisaka, T., and Yamanaka, S. (2009). Hypoxia enhances the generation of induced pluripotent stem cells. Cell Stem Cell *5*, 237-241.
Yu, M., Wei, Y., Xu, K., Liu, S., Ma, L., Pei, Y., Hu, Y., Liu, Z., Zhang, X., Wang, B., *et al*. (2019). EGFR deficiency leads to impaired self-renewal and pluripotency of mouse embryonic stem cells. PeerJ *7*, e6314.
Yun, M.H., Davaapil, H., and Brockes, J.P. (2015). Recurrent turnover of senescent cells during regeneration of a complex structure. Elife *4*.
Zaiss, D.M.W., Gause, W.C., Osborne, L.C., and Artis, D. (2015). Emerging functions of amphiregulin in orchestrating immunity, inflammation, and tissue repair. Immunity *42*, 216-226.
Zhang, C., Li, Y., Wu, Y., Wang, L., Wang, X., and Du, J. (2013). Interleukin-6/signal transducer and activator of transcription 3 (STAT3) pathway is essential for macrophage infiltration and myoblast proliferation during muscle regeneration. J Biol Chem *288*, 1489-1499.

FIGURE LEGEND

Figure 1. Senescence promotes *in vitro* reprogramming in a stress-dependent manner

A. Scheme of the experiments. **B & C.** Relative *in vitro* reprogramming efficiency of i4F MEFs exposed to secretome of non-senescent compared to senescent cells generated by different stress (corresponding to the respective controls: RS and IRIS to non-sen and OIS to vector alone). RS: replicative senescence, IRIS : γ-irradiation, OIS: oncogene-induced senescence. **B.** Co-culture system; Representative image of plate stained with alkaline phosphatase (AP) to reveal colonies arising from reprogramming (right panel). **C.** Conditioned medium system (CM). **D.** Reprogramming fold change of i4F MEFs cultured in different duration of OIS-CM before switching to Ctrl-CM. Scheme of the experiment (left panel). All the reprogramming fold changes was normalized to i4F in Ctrl-CM for 12

days, indicated by the blue dash line. Data correspond to the average ± s.d. using indicated n number of independent experiments. Statistical significance was assessed by ordinary one-way ANOVA test: *p < 0.05; **p < 0.01; **** p < 0.0001. See also **Figure S1**.

Figure 2. *in vivo* reprogramming in the skeletal muscle occurs normally in *Il6*$^{-/-}$ mice

A. Relative reprogramming efficiency of the i4F MEFs cultured in the CM derived from either WT or *Il6*$^{-/-}$ senescent cells. Senescence was induced using two different stresses, IRIS and OIS. Fold change was normalized with CM derived of respective non-senescent counterparts. **B.** Reprogramming efficiency of i4F MEFs cultured in CM of WT or *Il6*$^{-/-}$ senescent cells compared to treatment of IL-6 blocking antibody. Senescence was induced by over-expression of oncogene (OIS). Data correspond to the average ± s.d. using indicated n number of independent experiments. **C.** Transverse TA cryosections of indicated genotypes and sex after histological staining with Haematoxylin and Eosin (H&E). Dashed circle highlights dysplasia region. Scale bar: 50 μm. **D.** Experimental scheme (Upper panel) and quantification of **C.** The value represents one TA per mouse. Statistical significance was assessed by ordinary one-way ANOVA test: *p < 0.05; **p < 0.01; ***p < 0.001. See also **Figure S2.**

Figure 3. Proteomic analysis of oncogenic stress-induced secretome in *Il6*$^{-/-}$ MEFs

A. Fold change of reprogramming efficiency of i4F MEFs cultured in indicated different combination of various fractions of CM from non-senescent (Ctrl) or senescent (OIS) *Il6*$^{-/-}$. SN: supernatants (soluble proteins); sEV: small extracellular vesicles (exosome). Reprogramming efficiency fold change normalized to Ctrl-CM. Data correspond to the average ± s.d. using indicated n number of independent experiments. **B.** Volcano plot shows $\log_2$ fold change in protein intensity against the -log10 pvalue in SEN compared to Ctrl; blue dots are proteins with significant differential expression (FDR< 0.01). **C.** Summary of proteins either with significantly altered secretion (q-value < 0.01 and >2-fold change) by senescent (SEN) compared with quiescent cells (Ctrl), or exclusively detected in all repeats from one condition, following oncogenic stress (OIS) in senescent *Il6*$^{-/-}$ primary MEFs. **D.** ClueGO (Bindea et al., 2009) pathway enrichment and network analyses of OIS-secretome. Pathways of the same color have ⩾50% similarity. Connecting lines represent Kappa connectivity scores >

40%. Statistical significance was assessed by ordinary one-way ANOVA test: **p < 0.01. See also **Figure S3.**

Figure 4. AREG promotes *in vitro* reprogramming

A. Experimental scheme (upper panel). Fold change of reprogramming efficiency of i4F MEFs with different dosages of recombinant AREG protein. Normalized to Vehicle control (PBS). Representative image of plate stained with alkaline phosphatase (AP) to reveal colonies arising from reprogramming (right panel). **B.** Experimental scheme (upper panel). Comparison of reprogramming efficiency between PBS and recombinant AREG after different duration of DOX treatment. Data correspond to the average ± s.d. using indicated n number of independent experiments. **C-E.** Kinetics of expression of indicated genes at the indicated days during reprogramming comparing between PBS and AREG as measured by quantitative RT-PCR. Data correspond to the average ± s.e.m. of at least 2 independent assays. For each assay, qRT-PCR values were obtained in duplicate. Statistical significance was assessed by ordinary one-way ANOVA test for **A**, and two-way ANOVA test for **B-E:** *p < 0.05; **p < 0.01; ***p < 0.001. See also **Figure S4.**

Figure 5. AREG promotes *in vivo* reprogramming

A. Relative reprogramming efficiency of i4F MEFs treated with EGF (100ng/mL). Relative to PBS treated sample. **B.** Relative reprogramming efficiency of i4F MEFs with indicated treatment. Relative to PBS treated sample. Data correspond to the average ± s.d. of using indicated n number of different experiments using i4F MEFs generated from different embryos (A & B). **C.** Reprogramming efficiency of dermal fibroblasts derived from i4F mice with the indicated treatment and age. Data correspond to the average ± s.d. of using indicated n number of different MDF isolates. **D.** Experimental scheme for AREG administration during *in vivo* reprogramming. **E.** Representative TA sections with immunohistochemistry staining of anti-Nanog and histological staining of SAβGal of indicated treatment. Scale bar: 50 μm. **F.** Quantification of E. Data correspond to the average ± s.d. of using indicated n number of different mouse (average of two TA per mouse). Statistical significance

was assessed by the Mann-Whitney test (A) and ordinary one-way ANOVA (B, C, and F): *$p < 0.05$; **$p < 0.01$; ***$p < 0.001$. See also **Figure S5.**

Figure 1. Senescence promotes *in vitro* reprogramming in a stress-dependent manner

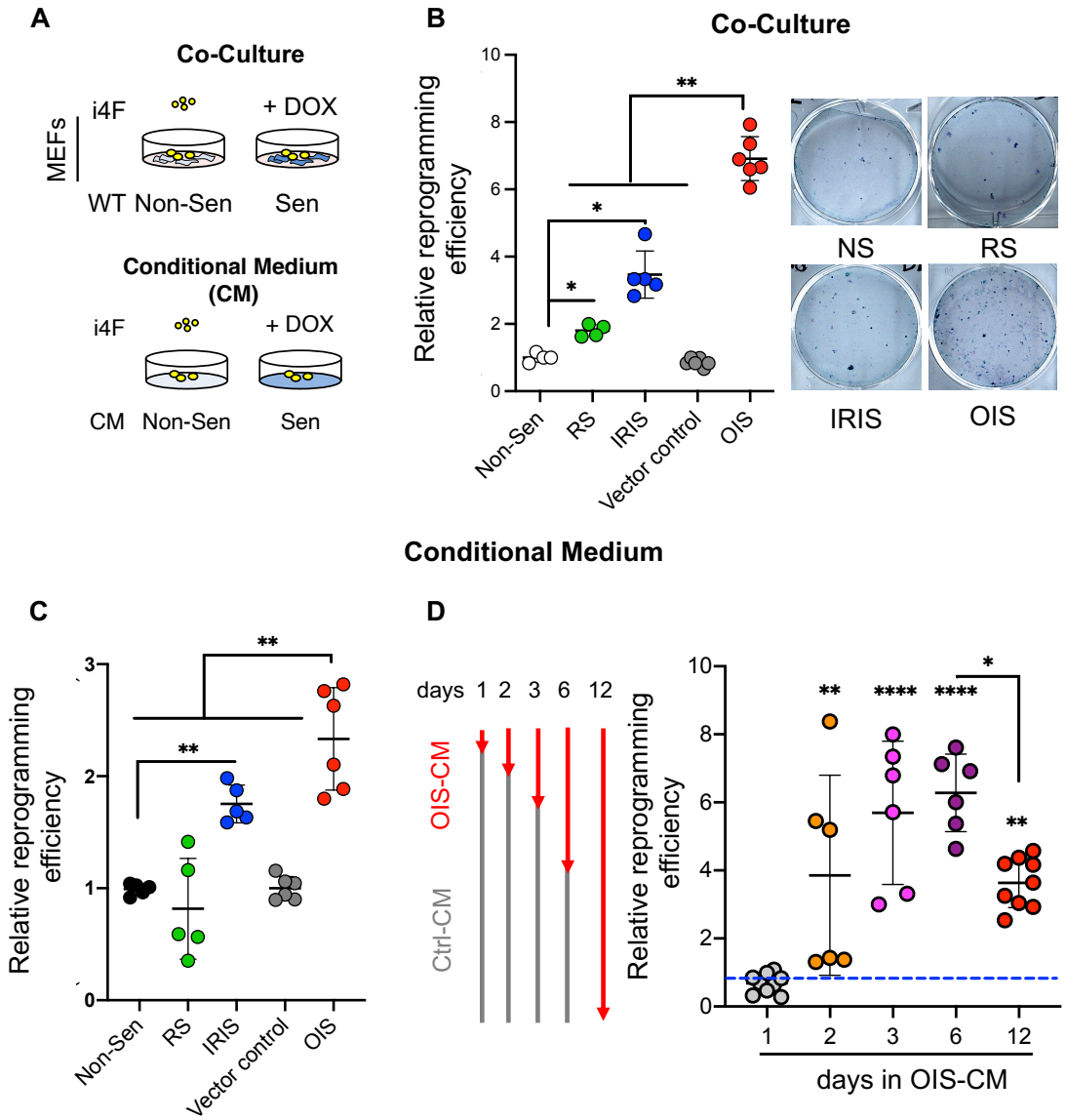

Figure 2. *in vivo* reprogramming in the skeletal muscle occurs normally in *Il6*$^{-/-}$ mice

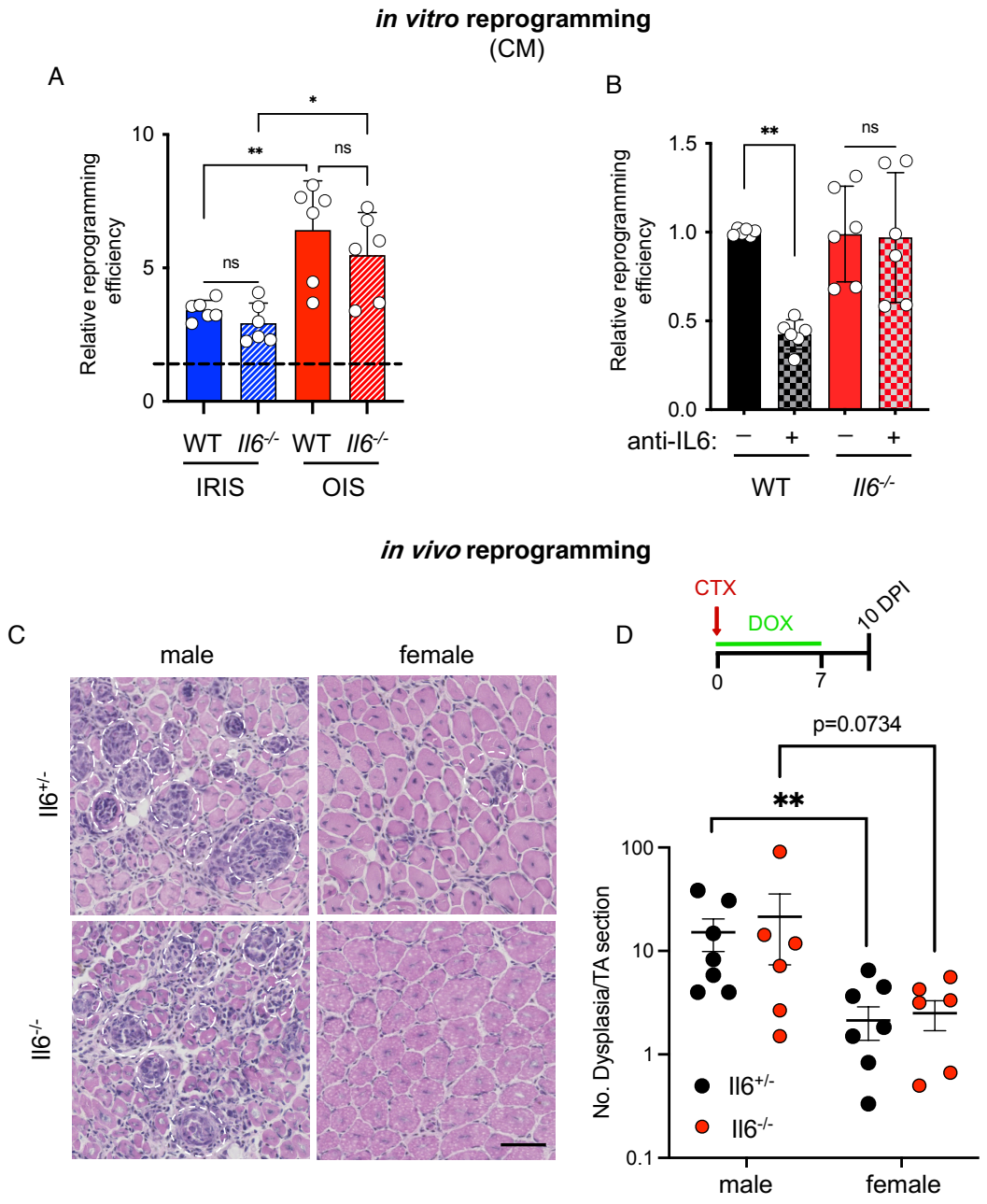

Figure 3. Proteomic analysis of oncogenic stress-induced secretome in *Il6*$^{-/-}$ MEFs

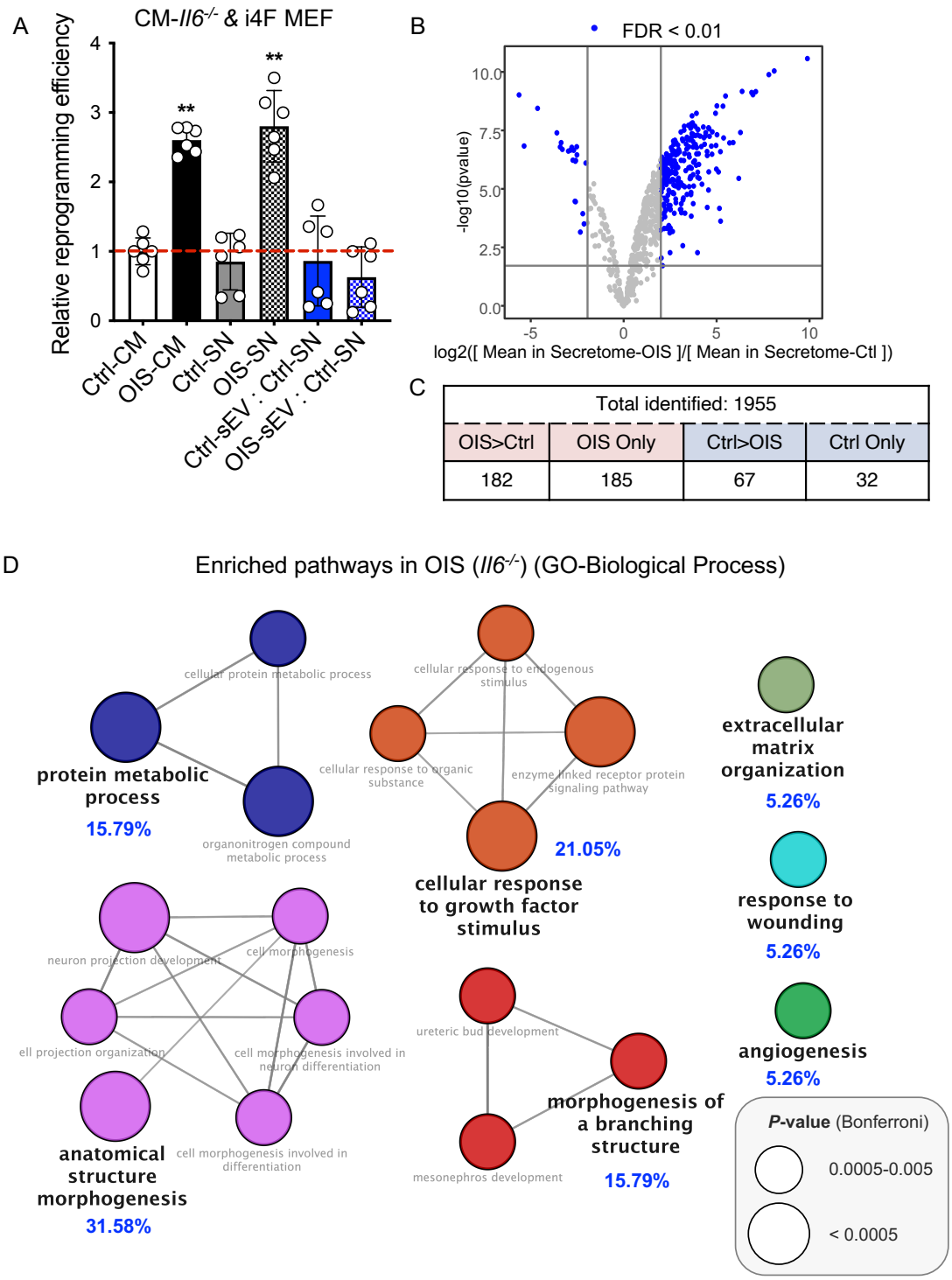

Figure 4. AREG promotes *in vitro* reprogramming

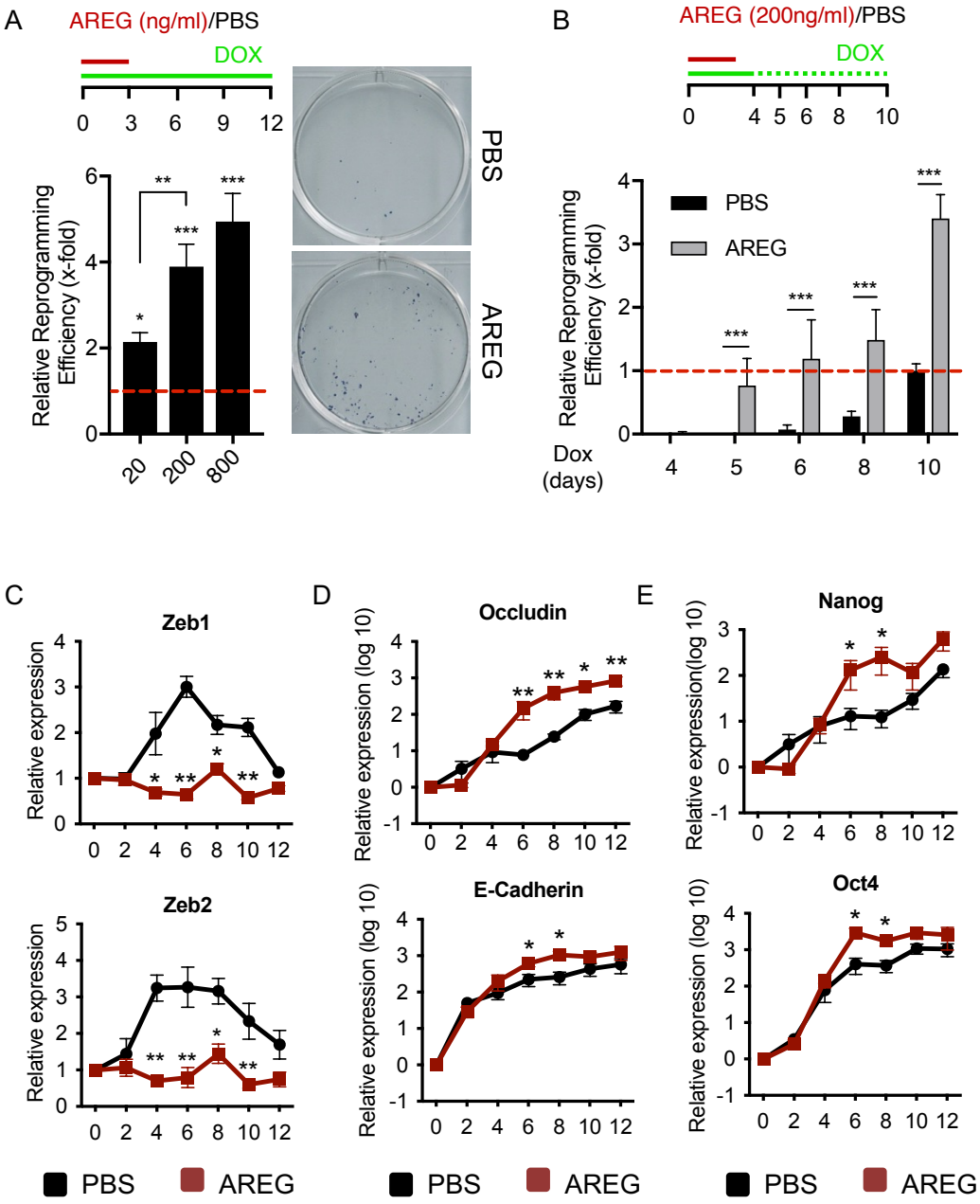
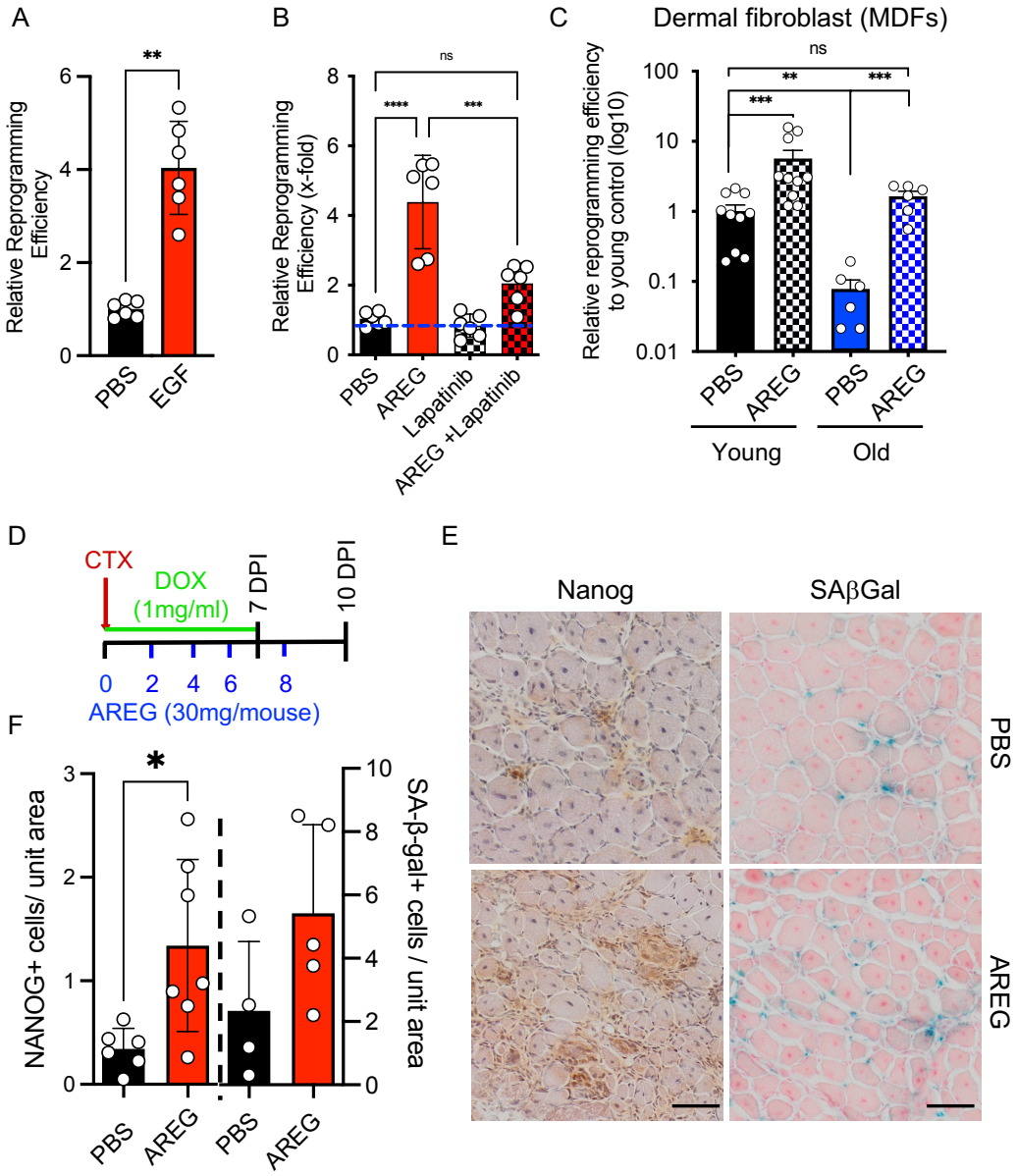
Figure 5. AREG promotes *in vivo* reprogramming